Hindawi Publishing Corporation
Advances in Meteorology
Volume 2014, Article ID 143917, 14 pages
http://dx.doi.org/10.1155/2014/143917

Research Article

The Influence of Topography on East African October to December Climate: Sensitivity Experiments with RegCM4

Bob Alex Ogwang,[1,2] Haishan Chen,[1] Xing Li,[1] and Chujie Gao[1]

[1] *Collaborative Innovation Center on Forecast and Evaluation of Meteorological Disasters, Key Laboratory of Meteorological Disaster, Ministry of Education, Nanjing 210044, China*
[2] *Uganda National Meteorological Authority, P.O. Box 7025, Kampala, Uganda*

Correspondence should be addressed to Haishan Chen; haishan@nuist.edu.cn

Received 1 July 2014; Accepted 16 September 2014; Published 21 October 2014

Academic Editor: Hann-Ming H. Juang

The influence of topography on east African climate is investigated using the International Centre for Theoretical Physics Regional Climate Model, with focus on October to December season. Results show that the mean rainfall (temperature) significantly reduces (increases) over the region when topography elevation is reduced. Based on the model, when topography over the selected region (KTU) is reduced to 25%, the mean rainfall (temperature) over east Africa is reduced (increased) by about 19% (1.4°C). The maximum rainfall (temperature) reduction (increase) is however observed around the region over which topography is reduced. The reduction in topography elevation resulted in an anomalous moisture divergence at low level and descending motion over the region. KTU topography enhances the surface heat flux over KTU region and tends to enhance convection over both KTU and the east African region. The topography also helps in the generation of the high frequency mesoscale and subsynoptic disturbances over the region. These disturbances produce precipitation over the region and may also enhance precipitation systems over remote areas due to propagation of the disturbances. The magnitude of the zonal wind speed at 850 hpa increases with the decrease in topography elevation.

1. Introduction

Topography plays an essential role in determining a planet's atmospheric circulation. It has long-range dynamical effects; a mountain can perturb a uniform flow to produce a train of waves downstream. It acts not only as an obstacle to the flow of air, but also as a source of heat. Variations in topography can establish horizontal temperature gradients which can generate a flow. Both dynamical and thermal manifestations of topography represent a problem of great complexity (Blumsack [1]).

The influence of topography (mountains) on different aspects of climate has been studied in different regions. Hahn and Manabe [2] noted that the influence of Tibetan Plateau (TP) on the south Asian monsoon circulation is attributed to mechanical and thermodynamic effects of TP. The presence of mountains is noted to be instrumental in maintaining the south Asian low pressure systems. Dickinson and Knight [3] studied the frontal interaction with mesoscale topography and showed that mountains retard and block the approaching front at the surface while the upper-level potential vorticity anomaly associated with the front moves across the domain unaffected.

Recent studies have made use of different models to examine the influence of topography on climate (e.g., Lee et al. [4] (Tibetan Plateau), [5, 6] (Rocky Mountains)). For example, Flesch and Reuter [6] noted that when topography elevation is reduced, rainfall amount reduces. The maximum reduction in rainfall amount is registered over the mountains and foothills and is associated with the reduction in orographic lifting and the associated vertical water vapor flux.

It has been noted that the seasonal rainfall patterns over east Africa are very complex due to the existence of complex topography and large inland water bodies (Indeje et al. [7]). Research on the influence of topography on the east African

climate is generally lacking. It thus calls for more research in this regard.

In the tropics where the domain of this study lies, the most important climate element is rainfall (Okoola [8]). In recent years, east Africa has suffered frequent events of both excessive [9, 10] and deficient rainfall (Hastenrath et al. [11]) which impacted negatively on the economy since most of the economic sectors largely depend on water resources. Rainfall variability and predictability are therefore important aspects to address in climate research, especially over the region. The patterns of rainfall (precipitation) over east Africa are generally controlled by the seasonal migration of the intertropical convergence zone (ITCZ) that migrates, north-south, across the region twice a year. The ITCZ thus tends to impose a significant influence on the climatological rainfall and temperature patterns. ITCZ influences and defines the bimodal rainfall regime experienced in most parts during March to May (MAM) and October to December (OND). Normally, the passage of ITCZ leads the onset of the two rainy seasons by 3 to 4 weeks, but this may be modulated from season to season by the interactions between the ITCZ and perturbations in the global climate circulation, as well as with changes in the local circulation systems initiated by land surface heterogeneity induced by variable vegetation characteristics, large inland lakes, and topography [12–14].

Seasonal forecasts or long-term climate projections are nonetheless reliant on the ability to resolve at a sufficiently high resolution, the detailed patterns of rainfall distribution. This question can be addressed via downscaling method. This method is particularly critical and a demanding exercise in east Africa. This is due to the complex topography, which includes several mountains and large lakes embedded in contrasted topographical settings. Alongside statistical methods, numerical simulations based on Regional Climate Models (RCMs) are increasingly being used to downscale atmospheric variables associated with large-scale climate forcing. RCMs have been widely used in different parts of the world to understand regional climate processes, seasonal climate variability, and regional climate change. Various versions of RCMs have so far been used in different regions [15–28].

Regional climate simulations previously dedicated to east Africa have mostly used the lower versions of the ICTP RCM [29–33]. Otieno and Anyah [34] investigated the effects of land use changes on climate using RegCM4.0, focusing over Kenya.

The use of RegCM4 is generally lacking over the east African region, especially in climate research. In this study, we use RegCM4.0 to investigate the influence of topography on east African climate, focusing on October to December season. A brief description of the model is given in Section 2. Section 3 provides data and model setup. Results and Discussion is given in Section 4, while Summary and Conclusion are given in Section 5.

2. Model Description

The Regional Climate Model (RegCM4) is the latest version of the Abdus Salam International Center for Theoretical Physics (ICTP) Regional Climate Model [35, 36]. It is an evolution of the previous version (RegCM3), described by Pal et al. [37]. The dynamical structure of RegCM4.0 is the same as that of the hydrostatic version of the mesoscale model, version 5 (MM5) of the National Center for Atmospheric Research (NCAR) and Pennsylvania State University (Grell et al. [38]). RegCM4.0 and the available model options are briefly summarized as follows.

It is a hydrostatic, compressible, sigma-p coordinate model run on Arakawa B-grid in which wind and thermodynamical variables are horizontally staggered (Giorgi et al. [39]). The radiative transfer scheme used is that of the global model CCM3 [40, 41]. The planetary boundary layer (PBL) used is the modified Holtslag (Holtslag et al. [42]) and a new PBL scheme of the University of Washington [43, 44] is implemented in the model.

Three cumulus convection schemes exist. The simplified version of the Kuo-type scheme of Anthes [45] is described by Anthes et al. [46] and has been present since the earliest version (RegCM1). The second and the mostly used scheme is that of Grell [47] in the implementation of Giorgi et al. [48]. Two different closure assumptions can be adopted (Arakawa-Schubert or Fritsch-Chappell). The third is the MIT scheme, introduced in RegCM3 [37, 49, 50].

The resolved scale precipitation scheme is essentially based on the SUBEX (subgrid explicit moisture scheme) parameterization of Pal et al. [51] and includes a prognostic equation for cloud water (the scheme is not significantly changed in RegCM4.0 compared to RegCM3, other than in some parameter settings).

The land surface processes are described via the Biosphere-Atmosphere Transfer Scheme (BATS) of Dickinson et al. [52], Subgrid BATS Giorgi et al. [53], and the Community Land Model version CLM3.5 [54, 55]. Compared to BATS, CLM is a more advanced package described in detail by [56, 57]. For the ocean fluxes, it makes use of the drag-coefficient parameterization included in the BATS package (Dickinson et al. [52]), and to improve the calculation of diurnal fluxes over the ocean, the prognostic sea surface temperature (SST) scheme described by Zeng and Beljaars [58] was implemented in the model. In RegCM3, Pal et al. [37] implemented the scheme of Zeng et al. [59] which is based on a Monin-Obhukov turbulence representation. This scheme was added in order to improve the excessive evaporation over warm tropical oceans found in the BATS option.

A simplified aerosol scheme specifically designed for application to long-term climate simulations has been incrementally developed within the RegCM system. Solmon et al. [60] first implemented a first-generation aerosol model including SO_2, sulfates, organic carbon, and black carbon. Zakey et al. [61] then added a 4-bin desert dust module, and Zakey et al. [62] implemented a 2-bin sea salt scheme. Additionally in RegCM4, the dust emission scheme accounts for subgrid emissions by different types of soil, and the soil texture distribution has been updated according to Laurent et al. [63]. The dust emission size distribution can now also be treated according to Kok [64]. When all aerosols are simulated, 12 additional prognostic equations are solved in RegCM4, including transport by resolvable scale winds,

Table 1: Model configuration used in the study.

Content	RegCM4.0
Resolution	50 km
Map projection	Normal Mercator
Horizontal dimension	192×110 ($j_x \times i_y$)
Vertical levels	18
Cumulus convection:	Grell (Grell, 1993 [47])
Planetary boundary layer	Holtslag et al. (1990 [42]), Bretherton et al. (2004 [44])
Microphysics	SUBEX (Pal et al. 2000 [51])
Land Surface Processes	CLM3.5 (Steiner et al. 2009 [54]; Tawfik and Steiner, 2011 [55])

turbulence and deep convection, sources, and wet and dry removal processes (Giorgi et al. [36]). The RegCM system includes an interactive 1-dimensional thermal lake model which has been applied in different regional settings, such as [65, 66]. The tropical band configuration is also implemented in RegCM4. In this configuration, the model uses a Mercator projection centered over the equator for a band covering the entire tropical region, from 45°S to 45°N. The use of the Mercator projection allows the model grid to exactly cover the tropical band with the end points in the longitudinal direction exactly overlapping (Coppola et al. [67]).

3. Data and Model Setup

In this study, Grell convection scheme with Fritsch-Chappell closure assumption (Grell-FC) is used, as in Sylla et al. [24]. Adeniyi [68] similarly observed that Grell-FC offers a better simulation over west Africa. The land surface processes are described via the Community Land Model, version CLM3.5. It is chosen based on the model performance in this particular domain, as in Yu and Wang [69]. The model was run at a resolution of 50 km (Table 1) over the period 1999–2008.

The experiments were done with the initial and lateral boundary conditions obtained from ERA-interim gridded reanalysis data at 1.5 degree resolution (Uppala et al. [70]). The data is a third generation of the European Centre for Medium-Range Weather Forecast (ECMWF) reanalysis product. The sea surface temperatures are obtained from the National Oceanic and Atmospheric Administration (NOAA). It is the Optimum Interpolated Sea Surface Temperature (OISST), produced weekly on a 1 degree resolution (Reynolds et al. [71]). The SST and the boundary conditions are updated 6 hourly in the model.

Three sets of experiments were done. The control experiment with actual topography (TP100) and sensitivity experiments with topography reduced to 75% (TP75) and 25% (TP25). The area over which topography is reduced lies between longitudes 34°E–38°E and latitudes 6°S–2°N. It will hereafter be referred to as KTU since it covers high mountains in parts of Kenya, Tanzania, and Uganda (KTU) including *Mt. Elgon, Mt. Kenya, Mt. Kilimanjaro, Mt. Meru, Usambara Range, and Ngorongoro Crater, among others.* Researchers such as those in [4–6] used a similar approach in their studies.

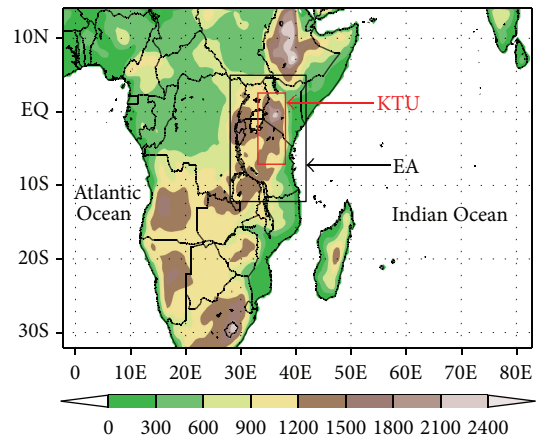

Figure 1: The model domain and elevation (in m). The rectangle (EA) is the area of study (east Africa), located over longitudes 28°E–42°E and latitudes 12°S–5°N. The inner rectangle (red) is the area (KTU) over which topography is reduced [34°E–38°E, 6°S–2°N] in the sensitivity experiments.

Precipitation datasets used to evaluate the model performance over east Africa are the Global Precipitation Climatology Project (GPCP) version 2.2 combined precipitation dataset, gridded at 2.5 degree resolution (Adler et al. [72]) provided by the NOAA/OAR/ESRL PSD, Boulder, Colorado, USA, from their web site at http://www.esrl.noaa.gov/psd/ and that of Climate Research Unit, CRU TS3.10 dataset [73, 74]. CRU TS3.10 (CRU TS 3.10.01 for precipitation) is a monthly gridded climatology of station data for the period 1901–2009 at a resolution of 0.5 degree. This is because the African rain-gauge data observed during the postindependence era of the 1970s through to recent years has many spatial and temporal discontinuities over large sections of east Africa (Schreck III and Semazzi [75]). The wind, relative humidity, and temperature used to determine and evaluate moisture transport are those of ERA-interim, gridded at 0.75 degree resolution (Dee et al. [76]). The National Centers for Environmental Prediction/National Center for Atmospheric Research (NCEP/NCAR) reanalysis zonal and meridional wind (Kalnay et al. [77]) were used to compute eddy kinetic energy. The first year of the model output was dropped as part of the model spin-up. Analyses were then done over 9 years (2000–2008).

4. Results and Discussion

In this section, the model results are provided and discussed. Figure 1 shows the model domain and elevation in meters, the study area (EA), and the region KTU over which topography is reduced in the sensitivity experiments.

4.1. Annual Cycle of Rainfall and Temperature. Under a changing climate, the annual cycle is expected to vary and thus the observed increasing intensity of global warming in recent years could significantly offset the subtle balance

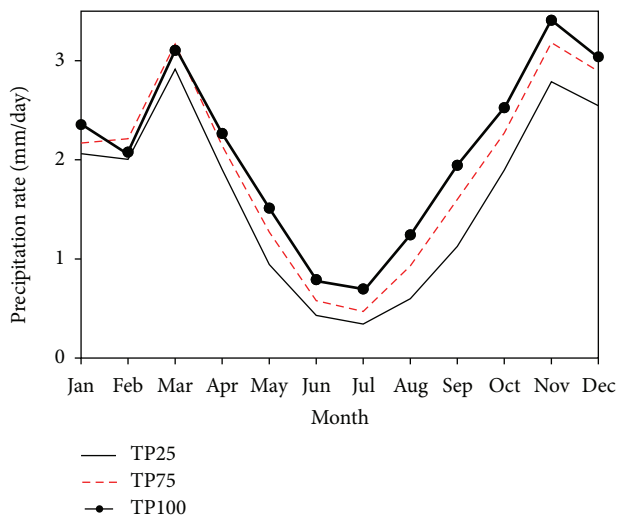

Figure 2: The mean annual cycle of precipitation (in mm/day) for the period 2000–2008, averaged over longitudes 28°E–42°E and latitudes 12°S-5°N. TP100 is due to the simulation with actual topography (control experiment), TP75 is due to the simulation with topography over KTU reduced to 75%, and TP25 represents simulation when the topography is reduced to 25%.

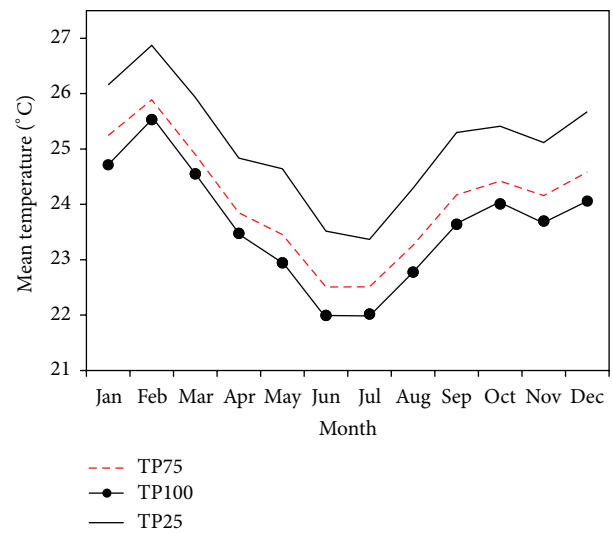

Figure 3: The mean annual cycle of the 2 m temperature (in °C) for the period 2000–2008, averaged over longitudes 28°E–42°E and latitudes 12°S–5°N. TP100 is due to the simulation with actual topography (control experiment), TP75 is due to the simulation with topography over KTU reduced to 75%, and TP25 represents simulation when the topography is reduced to 25%.

among the various climatological sources of climate variability over the region (Owiti and Zhu [14]). For example, in the period 1996 to 2005, 9 out of the 10 years are among the years with the highest annual temperature on record prior to the Intergovernmental Panel on Climate Change report (IPCC [78]). Knowledge of variability of rainfall and temperature in terms of annual cycle are therefore important components in the understanding of climate variability.

The climatology of the annual cycle is characterized by unimodal, bimodal, and trimodal rainfall regimes in different zones over east Africa (Section 1). However, the climatology of the observed area average annual cycle of rainfall over the region [28°E–42°E, 12°S–5°N] has higher amounts of rainfall received in October through May, with lower values received between June and September. This climatology is well captured by the model over the period 2000–2008 (Figure 2), where the simulation with actual topography (TP100 or control experiment) exhibits higher amount of rainfall received over east Africa, followed by simulation with the topography over the region KTU reduced to 75% (TP75). The least rainfall amounts are received when the topography is reduced further to 25% (TP25), implying that rainfall over the study area decreases with decreasing KTU topography. The presence of KTU topography thus enhances precipitation over the study area.

Analysis of the annual cycle of temperature (Figure 3) reveals that temperature generally increases with reducing topography over KTU.

4.2. Seasonal Rainfall and Temperature. As discussed in Section 1, the ITCZ is recognized for defining the bimodal rainfall regime experienced in most parts of the region during March to May (MAM) and October to December (OND). Rainfall is modulated from one season to another by the interaction between the ITCZ and perturbations in the global climate circulation, as well as with changes in the local circulation systems initiated by land surface heterogeneity induced by variable vegetation characteristics, large inland lakes, and topography (Owiti and Zhu [14]).

In this section, the influence of KTU topography on OND rainfall and temperature over east Africa is examined. Results (Figure 4) show that the model captures the observed pattern of OND rainfall (Figures 4(a) and 4(b)) over the region, with maximum rainfall over the western sector as opposed to the northeastern sector which tends to receive less rainfall. The sensitivity tests, Figures 4(c) and 4(d), reveal that there is a general reduction in rainfall in most parts of east Africa when topography over KTU is reduced to 25% (Figure 4(d)). There exists a significant reduction in rainfall around the region over which topography is reduced (Figure 4(g)), with a small section over northern Kenya (Turkana region) exhibiting an increase in rainfall. This corroborates the findings by Flesch and Reuter [6] that the maximum reduction in rainfall amounts is registered over the mountains and foothills. The reduction in rainfall is associated with the reduction in orographic lifting and the associated vertical water vapor flux (Flesch and Reuter [6]).

Further analysis of the remote influence of KTU topography in locations which are not part of KTU (Figure 11) reveals that the reduction in KTU elevation leads to a reduction in rainfall in locations UG (30°E–33°E, 1°N–4°N) and TZ (33°E–39°E, 10°S–7°S), whereas over KE (37°E–39°E, 3°N–5°N) there is an increase in rainfall, which agrees with the observed increase in Figure 4(g). KTU topography thus has influence on remote locations over east Africa.

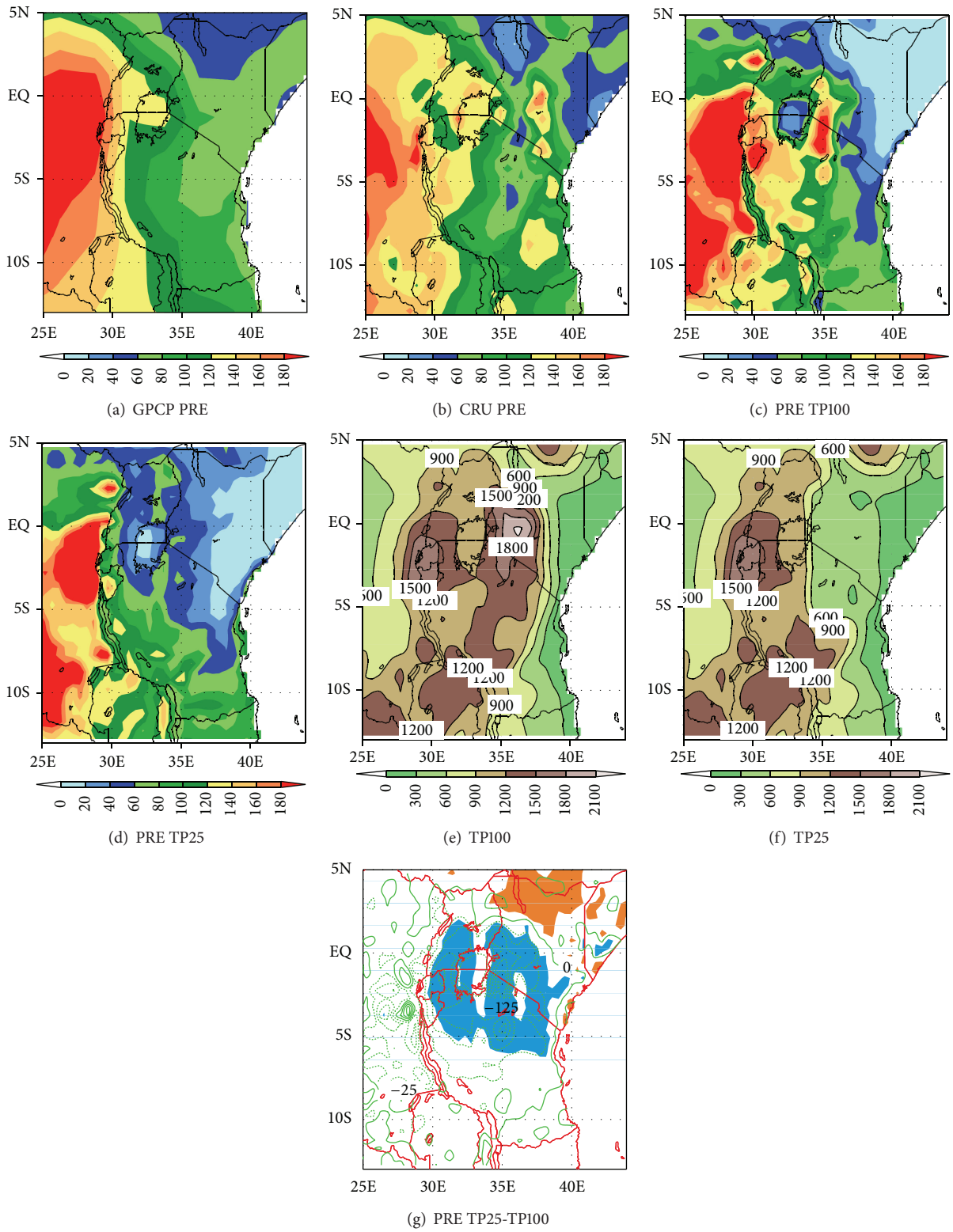

Figure 4: Climatology of OND rainfall (in mm) over the period 2000–2008: (a) GPCP observed rainfall, (b) CRU observed rainfall, (c) simulated using actual topography (TP100), (d) simulated using topography reduced to 25% (TP25) over 34°E–38°E and 6°S–2°N, (e) actual topography (TP100), (f) topography over KTU reduced to 25% (TP25), and (g) rainfall difference [(d) minus (c)] with contours (green) at 25 mm interval and the thick (black) contours represent regions over which the rainfall difference is zero. The shaded regions in (g) are significant at 95% confidence level (*where shaded blue* (*orange*) *implies decrease* (*increase*) *in rainfall*).

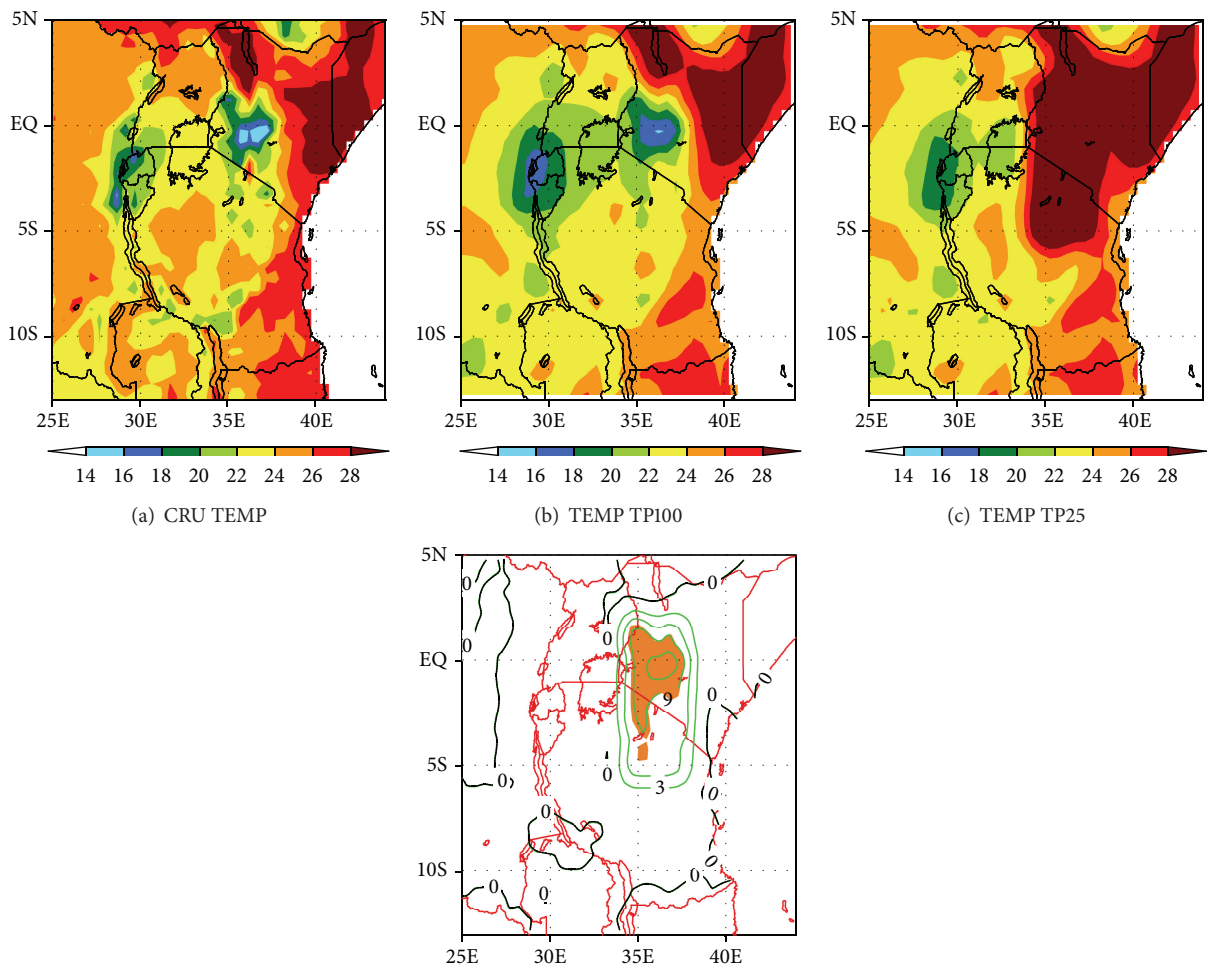

Figure 5: Climatology of OND 2 m temperature (in °C) over the period 2000–2008: (a) CRU observed temperature over land, (b) simulated using actual topography (TP100), (c) simulated using topography reduced to 25% (TP25) over 34°E–38°E and 6°S–2°N, and (d) temperature difference [(c) minus (b)] with contours (green) at 3°C interval and the thick (black) contours represent regions over which the temperature difference is zero. The shaded region in (d) is significant at 90% confidence level (*shaded area (orange) indicates a region of significant increase in temperature*).

In order to understand the influence of topography on the interannual variability of rainfall, we examine the standard deviation of the mean OND rainfall for the simulation with actual topography and that with topography reduced to 25%. Results (Figure 12) indicate that the standard deviation decreases over all the analysis regions, except KE region, which shows an increase when topography is reduced. This reveals that the interannual variability of rainfall over the region is similarly influenced by topography.

Analysis of OND temperature reveals that the model realistically reproduces the observed temperature (Figures 5(a) and 5(b)), with the highest temperature values observed in the northeastern sector of EA. Sensitivity tests (Figures 5(b) and 5(c)) show that there is a general increase in temperature in most parts of east Africa when topography over KTU is reduced to 25%. The maximum increase in temperature is observed in the region over which topography is reduced (Figure 5(d)). Further analysis reveals that the area average temperature over EA (KTU), Table 3, increases by about 1.4°C (8°C) when topography over KTU is reduced to 25%. The increase in temperature may also be associated with the observed reduction in rainfall over the region (Afiesimama et al. [79]).

4.3. Wind and Moisture Transport. Atmospheric circulation is important to precipitation because its ultimate effect is to increase the water vapor in the local air and lower the air temperature by transporting water vapor and invading cold air, leading to air saturation (Lu [80]). In order to offer possible explanation in regard to the observed reduction in rainfall over the region, we investigate the moisture transport at 850 hpa and the associated moisture convergence/divergence during OND season. The climatology of

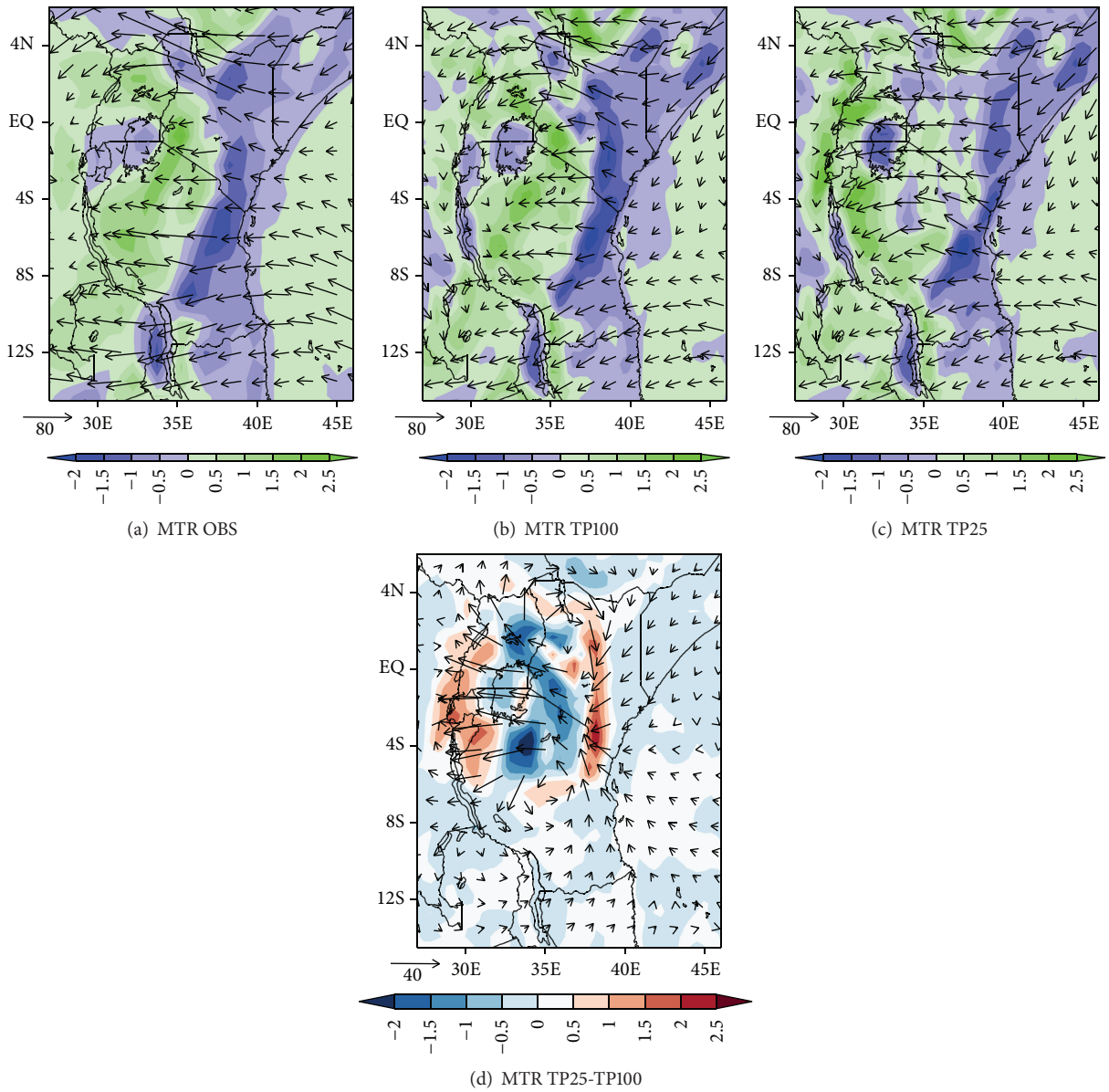

Figure 6: Climatology of OND water vapor/moisture transport (MTR) at 850 hpa in $g\,kg^{-1}\,ms^{-1}$ over the period 2000–2008. The shaded regions indicate moisture convergence (*positive*) and moisture divergence (*negative*), and the vectors show water vapor transport. (a) ERA interim reanalysis MTR, (b) simulated MTR using actual topography (TP100), (c) simulated MTR when KTU topography is reduced to 25%, and (d) difference in MTR [(c) minus (b)].

the observed moisture transport is characterized by a high moisture convergence to the east of Lake Victoria (around 35°E, 1°S), covering part of KTU (Figure 6(a)). This convergence is well captured by the control experiment (Figure 6(b)). However, in the sensitivity experiment where the topography over KTU is reduced to 25%, the high moisture convergence zone shifts to the west of Lake Victoria, around longitude 30°E. Figure 6(d) exhibits anomalous moisture divergence over most parts, with maximum divergence over the region between longitudes 33°E–37°E and latitudes 6°S–2°N, covering most parts of KTU where a significant rainfall reduction is observed.

The magnitude of the mean OND zonal wind speed (mainly easterlies) at 850 hpa over the EA region is observed to increase with decreasing topography elevation (Figure 7). This may be responsible for the observed shift in the maximum moisture convergence zone at this level from the east of Lake Victoria (around 35°E, 1°S) to far west.

Further analysis of the vertical velocity (omega) reveals that the climatology of OND omega is characterized by rising motion over the region (Figure 8(a)), particularly between longitudes 28°E–38°E (which includes KTU topography region). This climatology is realistically captured by the model when the actual topography is used (Figure 8(b)).

Table 2: Statistics of the model simulated mean OND rainfall (RF) in mm over east Africa (RF_EA), averaged over longitudes 28°E–42°E and latitudes 12°S–5°N, and that over KTU (RF_KTU), averaged over longitudes 34°E–38°E and latitudes 6°S–2°N for the control experiment (TP100), sensitivity experiments with topography reduced to 75% (TP75) and 25% (TP25), and the observed CRU and GPCP datasets. B_EA and B_KTU are the rainfall biases with respect to TP100, over EA and KTU, respectively. The respective percentage biases due to EA and KTU are denoted by PB_EA and PB_KTU.

	RF_EA (mm)	RF_KTU (mm)	B_EA (mm)	B_KTU (mm)	PB_EA	PB_KTU
GPCP	96.0	80.1				
CRU	101.1	90.4				
TP100	91.6	92.0				
TP75	85.2	67.8	−6.4	−24.2	−7%	−26%
TP25	73.8	36.7	−17.8	−55.3	−19%	−60%

Table 3: Statistics of the model simulated mean OND temperature (Tm in °C) over east Africa (Tm*EA), averaged over 28°E–42°E, 12°S–5°N and that over KTU (Tm*KTU), averaged over longitudes 34°E–38°E and latitudes 6°S–2°N for the control experiment (TP100), sensitivity experiments with topography reduced to 75% (TP75) and 25% (TP25), and the observed CRU data. B*EA and B*KTU are temperature biases over EA and KTU, respectively, with respect to TP100.

	Tm*EA (°C)	Tm*KTU (°C)	B*EA (°C)	B*KTU (°C)
CRU	24.4	22.1		
TP100	24.0	21.7		
TP75	24.5	24.3	0.5	2.6
TP25	25.4	29.7	1.4	8.0

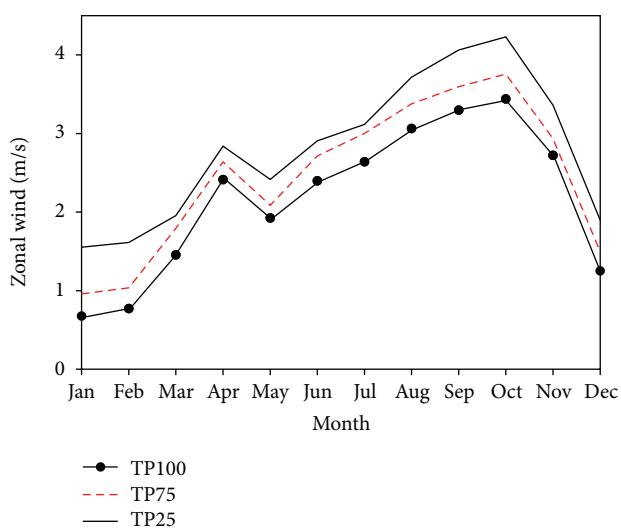

Figure 7: The mean annual cycle of the zonal wind magnitude (in ms^{-1}) for the period 2000–2008, averaged over longitudes 28°E–42°E and latitudes 12°S–5°N. TP100 is due to the simulation with actual topography, TP75 is due to the simulation with topography reduced to 75%, and TP25 represents simulation when the topography is reduced to 25%.

When KTU topography is reduced to 25% (Figure 8(c)), the rising motion is suppressed. This implies that the observed rising motion over the region is associated with orographic lifting due to KTU topography.

The vertical velocity difference [(c) minus (b)] in Figure 8(d) shows that there is a net subsidence over the region. The anomalous sinking motion indicates that convection is suppressed as a result of reducing topography to 25%. According to Flesch and Reuter [6], the reduction in rainfall is associated with the reduction in orographic lifting and the associated vertical water vapor flux. It thus explains why rainfall over KTU reduced (by about 60%), which in turn reduced the area average rainfall amount recorded in the entire region of east Africa by about 19% (Table 2).

According to Shi et al. [5], the activities of high frequency mesoscale and subsynoptic disturbances can be measured by the eddy kinetic energy (EKE) in the simulations. EKE is defined as

$$\mathrm{EKE} = \frac{1}{2}\left[(u-\overline{u})^2 + (v-\overline{v})^2\right], \quad (1)$$

where u and v are zonal and meridional wind components at 500 hPa and $\overline{u}$ and $\overline{v}$ are their respective time means. In order to examine the contribution of topography in the generation of the high frequency mesoscale and subsynoptic disturbances over the region, we compute EKE based on November 2006 (wet year) with the time mean values determined over the period 2000–2008. Results (Figure 10) indicate that the simulation with actual topography (TP100, Figure 10(b)) has a zonally oriented high EKE band between 28°E–43°E and 10°S–3°S (covering the southern sector of KTU), signifying active high frequency mesoscale and subsynoptic disturbances during the simulation period. On the other hand, when topography elevation is reduced to 25% (TP25, Figure 10(c)), a similar high EKE band appears, but the absolute values are much lower, indicating a suppression of the mesoscale and subsynoptic activities. The NCEP reanalysis generally underestimates the EKE (Figure 10(a)) due to the relative coarse resolution, as in Shi et al. [5].

TP100 experiment shows that the high frequency mesoscale and subsynoptic disturbances spread over most parts of east Africa, which produces precipitation in the region and may enhance precipitation systems over other regions as they propagate downstream to the inner sectors of east Africa.

4.4. Surface Heat Fluxes. In order to understand the thermal influence of topography over the region, we examine the response of surface heat flux in association with the observed rainfall anomaly due to the reduction in topography.

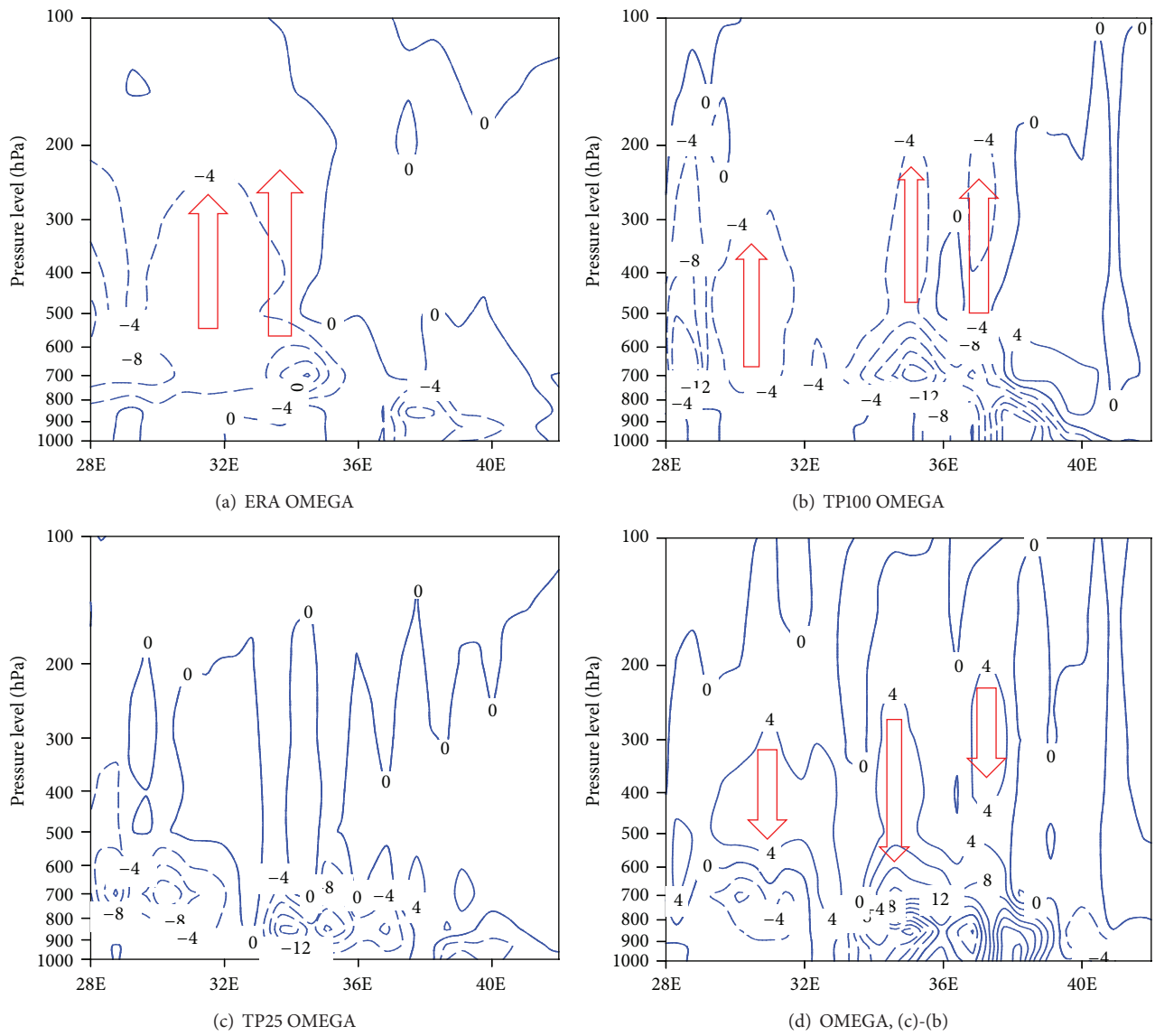

Figure 8: Climatology of OND vertical velocity (omega $\times 10^{-2}$ Pas^{-1}), averaged over latitudes 6°S–2°N for the period 2000–2008: (a) ERA interim reanalysis data, (b) simulated with actual topography (TP100 or control experiment), (c) simulated with topography over KTU reduced to 25%, and (d) difference between (c) and (b) [(c) minus (b)]. *Contours are at* 4×10^{-2} Pas^{-1} *interval.*

As shown in Figure 9(a), the surface (sensible and latent) heat flux is generally larger in the control experiment (TP100) than in the sensitivity experiment (TP25), particularly over KTU region where the maximum heat flux is observed.

Figure 9(b) shows that the sensible heat flux increases over the region between latitudes 5°S–2°N when topography is reduced to 25% (SHF is more in TP25 than in TP100), implying that the sensible heat flux increases with decreasing topography elevation over this region. However, over the region between longitudes 35°E–42°E and latitudes 2°N–5°N, the sensible heat flux is greater in TP100 than in TP25. This coincides with the observed significant increase in rainfall in this region (Figure 4(g)), resulting from the reduction in topography.

Analysis of the surface latent heat flux (LHF, Figure 9(c)) over the region reveals that LHF in TP100 is higher than LHF in TP25, implying that LHF deceases when topography is reduced. This is consistent with the observed reduction in rainfall over KTU region due to the reduction in topography. On the other hand, over the region between longitudes 35°E–42°E and latitudes 2°N–5°N, the latent heat flux is greater in TP25 than in TP100. This shows that LHF increases over this region as KTU topography is reduced. The increase in LHF over this region is similarly consistent with the observed increase in rainfall in the region (Figure 4(g)).

Generally, the presence of topography over KTU in TP100 experiment enhances the surface heat flux over KTU. This may enhance convection both over KTU and the region and

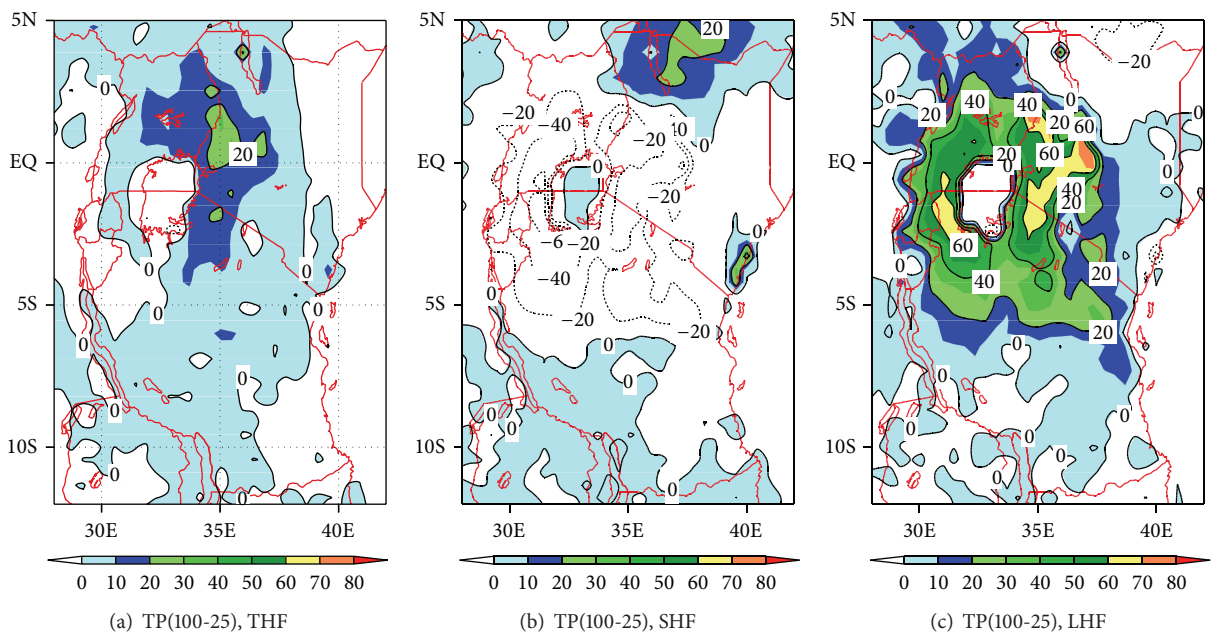

Figure 9: Spatial distributions of the mean OND differences (in W m^{-2}): (a) total surface (sensible + latent heat) fluxes (THF), (b) sensible heat flux (SHF), and (c) latent heat flux (LHF) between the control (TP100) and sensitivity (TP25) experiments averaged over the period 2000–2008. *The contour interval is* 20 Wm^{-2}.

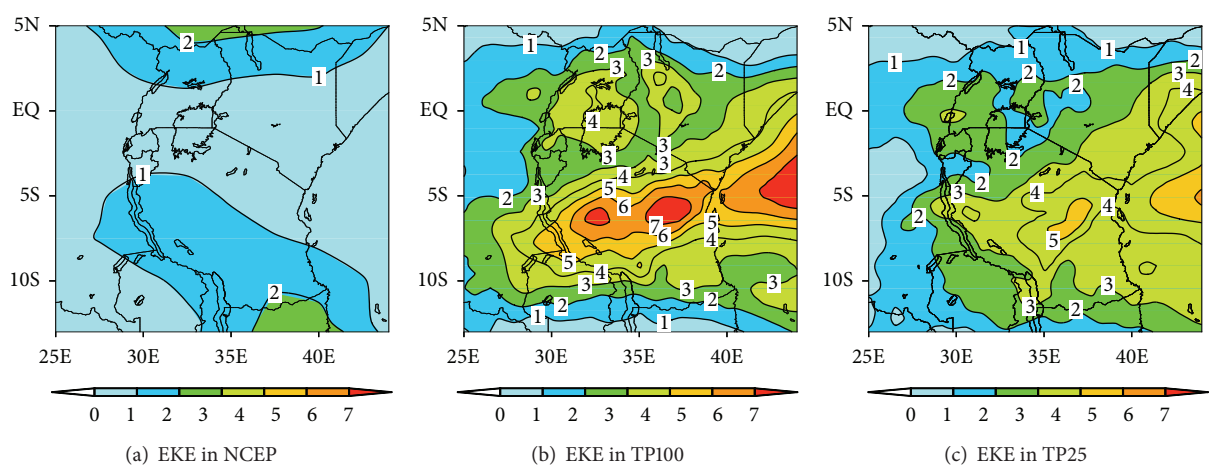

Figure 10: Spatial distributions of eddy kinetic energy (EKE in m^2 s^2) at 500 hPa, averaged during November 2006 from (a) NCEP reanalysis data, (b) control experiment with actual topography (TP100), and (c) sensitivity experiment with topography elevation reduced to 25% (TP25).

could explain why rainfall over the region is higher in TP100 than in TP25, as in Shi et al. [5].

5. Summary and Conclusion

In this study, we use the International Centre for Theoretical Physics (ICTP) Regional Climate Model (RegCM4.0) to examine the influence of topography on the east African climate, with focus on October to December (OND) season. The control simulation was done with actual topography and sensitivity experiments were carried out with topography elevation reduced to 75% and 25%.

Results show that the OND rainfall (temperature) significantly reduces (increases) over the region when topography elevation is reduced. Based on the model, when the topography over KTU is reduced to 25%, the mean OND rainfall (temperature) over EA region reduces (increases) by about 19% (1.4°C). The maximum rainfall (temperature) reduction (increase) is, however, observed around KTU region, where rainfall (temperature) over KTU reduces (increases) by about 60% (8°C). This may be explained by the anomalous moisture divergence exhibited over the region at low level and the associated anomalous sinking motion. Divergence at low level results in vertical shrinking which suppresses convection due to subsidence [81, 82].

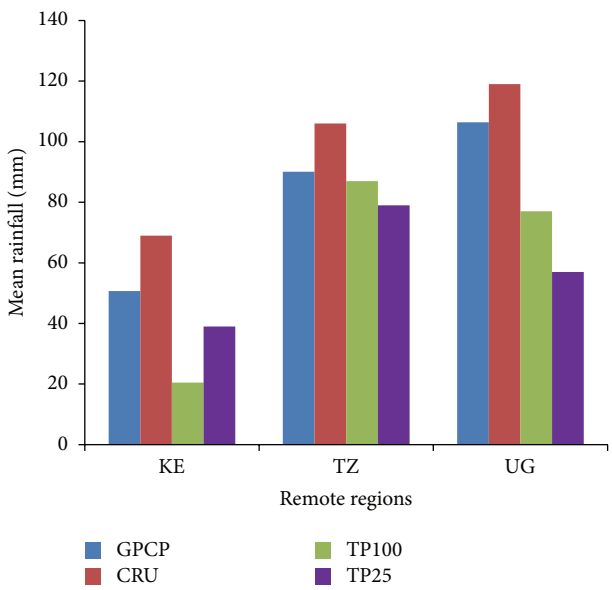

Figure 11: The mean OND rainfall (mm) over selected regions which are not part of KTU, refered to as remote regions, averaged over KE (37°E–39°E, 3°N–5°N) in Kenya, TZ (33°E–39°E, 10°S–7°S) in Tanzania, and UG (30°E–33°E, 1°N–4°N) in Uganda. TP100 is due to the simulation with actual topography, TP25 represents simulation when the topography is reduced to 25%, CRU refers to the Climate Research Unit data, and GPCP is the Global Precipitation Climatology Project data.

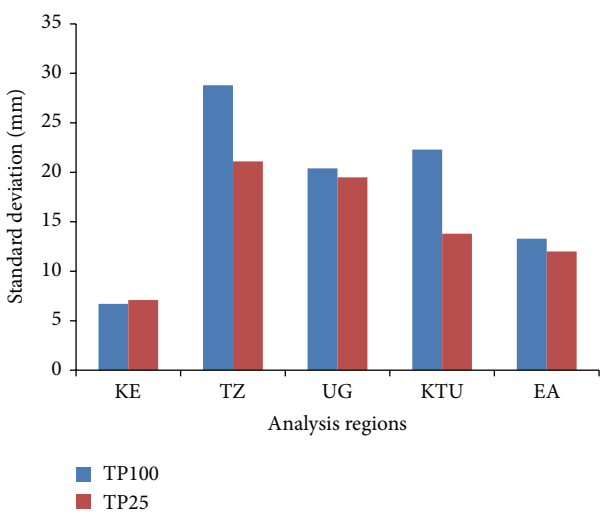

Figure 12: Standard deviation of the mean OND rainfall (mm) for the period 2000–2008, averaged over KTU, remote regions (KE, TZ, and UG, defined in Figure 11), and EA (28°E–42°E, 12°S–5°N). TP100 is due to the simulation with actual topography and TP25 represents simulation when the topography is reduced to 25%.

The interannual variability of OND rainfall over the east African region is influenced by KTU topography.

The presence of topography over KTU enhances the surface heat flux over the region.

The reduction in topography leads to an increase in the magnitude of the zonal wind speed (easterlies) at 850 hpa.

The eddy kinetic energy (EKE) shows that topography over KTU helps in the generation of the high frequency mesoscale and subsynoptic disturbances over the region. These disturbances produce precipitation over the region and also enhance precipitation systems over remote areas as a result of the propagation of the disturbances downstream.

The findings from this study and the biases identified call for more detailed investigative studies, particularly in the region. These results may motivate researchers and modeling centers to further improve the performance of the model over east Africa.

Disclosure

Bob Alex Ogwang is the first author.

Conflict of Interests

The authors declare that there is no conflict of interests regarding the publication of this paper.

Acknowledgments

The authors thank NOAA for providing the OISST data, ECMWF for providing the ERA-Interim reanalysis data, and the University of East Anglia Climatic Research Unit for the data used in this study. This study has been jointly supported by NSFC (41230422), the Special Funds for Public Welfare of China (GYHY 201206017), NCET Program, the Natural Science Foundation of Jiangsu Province of China under Grant no. BK2004001, and Project Funded by the Priority Academic Program Development of Jiangsu Higher Education Institutions (PAPD). The authors also thank Chinese Scholarship Council (CSC) for the financial support and Nanjing University of Information Science and Technology for providing the required facilities for data analysis and for all other forms of support.

References

[1] S. L. Blumsack, "On the effects of topography on Planetary Atmospheric Circulation," *Journal of Atmospheric Sciences*, vol. 28, pp. 1134–1143, 1971.

[2] D. G. Hahn and S. Manabe, "The role of mountains in the south Asian monsoon circulation," *Journal of the Atmospheric Sciences*, vol. 32, no. 8, pp. 1515–1541, 1975.

[3] M. J. Dickinson and D. J. Knight, "Frontal interaction with mesoscale topography," *Journal of the Atmospheric Sciences*, vol. 56, no. 20, pp. 3544–3559, 1999.

[4] S.-S. Lee, J.-Y. Lee, K.-J. Ha et al., "Role of the tibetan plateau on the annual variation of mean atmospheric circulation and storm-track activity," *Journal of Climate*, vol. 26, no. 14, pp. 5270–5286, 2013.

[5] X. Shi, Y. Wang, and X. Xu, "Effect of mesoscale topography over the Tibetan Plateau on summer precipitation in China: a regional model study," *Geophysical Research Letters*, vol. 35, no. 19, 2008.

[6] T. K. Flesch and G. W. Reuter, "WRF model simulation of two Alberta flooding events and the impact of topography," *Journal of Hydrometeorology*, vol. 13, no. 2, pp. 695–708, 2012.

[7] M. Indeje, F. H. M. Semazzi, and L. J. Ogallo, "ENSO signals in East African rainfall seasons," *International Journal of Climatology*, vol. 20, no. 1, pp. 19–46, 2000.

[8] R. E. Okoola, "Midtropospheric circulation patterns associated with extreme dry and wet episodes over equatorial Eastern Africa during the Northern Hemisphere spring," *Journal of Applied Meteorology*, vol. 38, no. 8, pp. 1161–1169, 1999.

[9] P. J. Webster, A. M. Moore, J. P. Loschnigg, and R. R. Leben, "Coupled ocean-atmosphere dynamics in the Indian Ocean during 1997-98," *Nature*, vol. 401, no. 6751, pp. 356–360, 1999.

[10] M. Latif, D. Dommenget, M. Dima, and A. Grötzner, "The role of Indian Ocean sea surface temperature in forcing east African rainfall anomalies during December-January 1998," *Journal of Climate*, vol. 12, no. 12, pp. 3497–3504, 1999.

[11] S. Hastenrath, D. Polzin, and C. Mutai, "Diagnosing the 2005 drought in equatorial East Africa," *Journal of Climate*, vol. 20, no. 18, pp. 4628–4637, 2007.

[12] T. D. Davies, C. E. Vincent, and A. K. C. Beresford, "July-August rainfall in west-central Kenya," *Journal of Climatology*, vol. 5, no. 1, pp. 17–33, 1985.

[13] C. C. Mutai, M. N. Ward, and A. W. Colman, "Towards the prediction of the East Africa short rains based on sea-surface temperature-atmosphere coupling," *International Journal of Climatology*, vol. 18, no. 9, pp. 975–997, 1998.

[14] Z. Owiti and W. Zhu, "East African rainfall seasonality based on modulated annual cycle (MAC)," *International Journal of Physical Science*, vol. 7, no. 24, pp. 3050–3061, 2012.

[15] M. R. Marinucci, F. Giorgi, M. Beniston et al., "High resolution simulations of January and July climate over the western Alpine region with a nested Regional Modeling system," *Theoretical and Applied Climatology*, vol. 51, no. 3, pp. 119–138, 1995.

[16] A. H. Lynch, W. L. Chapman, J. E. Walsh, and G. Weller, "Development of a regional climate model of the western Arctic," *Journal of Climate*, vol. 8, no. 6, pp. 1555–1570, 1995.

[17] A. Seth and F. Giorgi, "The effects of domain choice on summer precipitation simulation and sensitivity in a regional climate model," *Journal of Climate*, vol. 11, no. 10, pp. 2698–2712, 1998.

[18] X. Gao, Z. Zhao, Y. Ding, R. Huang, and F. Giorgi, "Climate change due to greenhouse effects in China as simulated by a regional climate model," *Advances in Atmospheric Sciences*, vol. 18, no. 6, pp. 1223–1229, 2001.

[19] X. Gao, Y. Xu, Z. Zhao, J. S. Pal, and F. Giorgi, "On the role of resolution and topography in the simulation of East Asia precipitation," *Theoretical and Applied Climatology*, vol. 86, no. 1–4, pp. 173–185, 2006.

[20] F. Giorgi, X. Bi, and J. S. Pal, "Mean, interannual variability and trends in a regional climate change experiment over Europe. I. Present-day climate (1961–1990)," *Climate Dynamics*, vol. 22, no. 6-7, pp. 733–756, 2004.

[21] B. J. Abiodun, J. S. Pal, E. A. Afiesimama, W. J. Gutowski, and A. Adedoyin, "Simulation of West African monsoon using RegCM3 Part II: impacts of deforestation and desertification," *Theoretical and Applied Climatology*, vol. 93, no. 3-4, pp. 245–261, 2008.

[22] R. Song, X. Gao, H. Zhang, and A. Moise, "20 km resolution regional climate model experiments over Australia: experimental design and simulations of current climate," *Australian Meteorological Magazine*, vol. 57, no. 3, pp. 175–193, 2008.

[23] M. Ashfaq, Y. Shi, W.-W. Tung et al., "Suppression of south Asian summer monsoon precipitation in the 21st century," *Geophysical Research Letters*, vol. 36, no. 1, Article ID L01704, 2009.

[24] M. B. Sylla, E. Coppola, L. Mariotti et al., "Multiyear simulation of the African climate using a regional climate model (RegCM3) with the high resolution ERA-interim reanalysis," *Climate Dynamics*, vol. 35, no. 1, pp. 231–247, 2010.

[25] T. Ozturk, H. Altinsoy, M. Türkeş, and M. L. Kurnaz, "Simulation of temperature and precipitation climatology for the Central Asia CORDEX domain using RegCM 4.0," *Climate Research*, vol. 52, no. 1, pp. 63–76, 2012.

[26] G. T. Diro, S. A. Rauscher, F. Giorgi, and A. M. Tompkins, "Sensitivity of seasonal climate and diurnal precipitation over Central America to land and sea surface schemes in RegCM4," *Climate Research*, vol. 52, no. 1, pp. 31–48, 2012.

[27] L. Zou and T. Zhou, "Improve the simulation of western North Pacific summer monsoon in RegCM3 by suppressing convection," *Meteorology and Atmospheric Physics*, vol. 121, no. 1-2, pp. 29–38, 2013.

[28] L. Zou and T. Zhou, "Near future (2016-40) summer precipitation changes over China as projected by a regional climate model (RCM) under the RCP8.5 emissions scenario: comparison between RCM downscaling and the driving GCM," *Advances in Atmospheric Sciences*, vol. 30, no. 3, pp. 806–818, 2013.

[29] L. Sun, F. H. M. Semazzi, F. Giorgi, and L. Ogallo, "Application of the NCAR regional climate model to eastern Africa 1. Simulation of the short rains of 1988," *Journal of Geophysical Research D: Atmospheres*, vol. 104, no. 6, pp. 6529–6548, 1999.

[30] L. Sun, F. H. M. Semazzi, F. Giorgi, and L. Ogallo, "Application of the NCAR regional climate model to eastern Africa, Part II: simulation of interannual variability of short rains," *Journal of Geophysical Research D*, vol. 104, no. 6, pp. 6549–6562, 1999.

[31] R. O. Anyah and F. H. M. Semazzi, "Simulation of the sensitivity of Lake Victoria basin climate to lake surface temperatures," *Theoretical and Applied Climatology*, vol. 79, no. 1-2, pp. 55–69, 2004.

[32] N. Davis, J. Bowden, F. Semazzi, L. Xie, and B. Önol, "Customization of RegCM3 Regional Climate Model for eastern Africa and a tropical Indian Ocean domain," *Journal of Climate*, vol. 22, no. 13, pp. 3595–3616, 2009.

[33] R. O. Anyah and F. H. M. Semazzi, "Variability of East African rainfall based on multiyear RegCM3 simulations," *International Journal of Climatology*, vol. 27, no. 3, pp. 357–371, 2007.

[34] V. O. Otieno and R. O. Anyah, "Effects of land use changes on climate in the Greater Horn of Africa," *Climate Research*, vol. 52, no. 1, pp. 77–95, 2012.

[35] F. Giorgi and R. O. Anyah, "The road towards RegCM4," *Climate Research*, vol. 52, no. 1, pp. 3–6, 2012.

[36] F. Giorgi, E. Coppola, F. Solmon et al., "RegCM4: model description and preliminary tests over multiple CORDEX domains," *Climate Research*, vol. 52, no. 1, pp. 7–29, 2012.

[37] J. S. Pal, F. Giorgi, X. Bi et al., "Regional climate modeling for the developing world: the ICTP RegCM3 and RegCNET," *Bulletin of the American Meteorological Society*, vol. 88, no. 9, pp. 1395–1409, 2007.

[38] G. Grell, J. Dudhia, and D. R. Stauffer, "A description of the fifth generation Penn State/NCAR Mesoscale Model (MM5)," National Center for Atmospheric Research Tech Note NCAR/TN-398+STR, National Center for Atmospheric Research, Boulder, Colo, USA, 1994.

[39] F. Giorgi, M. R. Marinucci, G. T. Bates, and G. De Canio, "Development of a second-generation regional climate model (RegCM2). Part II: convective processes and assimilation of lateral boundary conditions," *Monthly Weather Review*, vol. 121, no. 10, pp. 2814–2832, 1993.

[40] J. T. Kiehl, G. B. Bonan, B. A. Boville, B. P. Briegleb, D. L. Williamson, and P. J. Rasch, "Description of the NCAR community climate model (CCM3)," NCAR Technical Note TN-420 + STR, National Center for Atmospheric Research, Boulder, Colorado, 1996.

[41] F. Giorgi, Y. Huang, K. Nishizawa, and C. Fu, "A seasonal cycle simulation over eastern Asia and its sensitivity to radiative transfer and surface processes," *Journal of Geophysical Research D: Atmospheres*, vol. 104, no. 6, pp. 6403–6423, 1999.

[42] A. A. M. Holtslag, E. I. F. De Bruijn, and H.-L. Pan, "A high resolution air mass transformation model for short-range weather forecasting," *Monthly Weather Review*, vol. 118, no. 8, pp. 1561–1575, 1990.

[43] H. Grenier and C. S. Bretherton, "A moist PBL parameterization for large-scale models and its application to subtropical cloud-topped marine boundary layers," *Monthly Weather Review*, vol. 129, no. 3, pp. 357–377, 2001.

[44] C. S. Bretherton, J. R. McCaa, and H. Grenier, "A new parameterization for shallow cumulus convection and its application to marine subtropical cloud-topped boundary layers. Part I: description and 1D results," *Monthly Weather Review*, vol. 132, no. 4, pp. 864–882, 2004.

[45] R. A. Anthes, "A cumulus parameterization scheme utilizing a one-dimensional cloud model," *Monthly Weather Review*, vol. 105, pp. 1423–1438, 1977.

[46] R. A. Anthes, E. Y. Hsie, and Y. H. Kuo, "Description of the Penn State/NCAR Mesoscale Model Version 4 (MM4)," National Center for Atmospheric Research Tech Note TN-282+STR, NCAR, Boulder, Colo, USA, 1987.

[47] G. A. Grell, "Prognostic evaluation of assumptions used by cumulus parameterizations," *Monthly Weather Review*, vol. 121, no. 3, pp. 764–787, 1993.

[48] F. Giorgi, M. R. Marinucci, G. T. Bates, and G. de Canio, "Development of a second-generation regional climate model (RegCM2). Part II: convective processes and assimilation of lateral boundary conditions," *Monthly Weather Review*, vol. 121, no. 10, pp. 2814–2832, 1993.

[49] K. A. Emanuel, "A scheme for representing cumulus convection in large-scale models," *Journal of the Atmospheric Sciences*, vol. 48, no. 21, pp. 2313–2335, 1991.

[50] K. A. Emanuel and M. Živković-Rothman, "Development and evaluation of a convection scheme for use in climate models," *Journal of the Atmospheric Sciences*, vol. 56, no. 11, pp. 1766–1782, 1999.

[51] J. S. Pal, E. E. Small, and E. A. B. Eltahir, "Simulation of regional-scale water and energy budgets: representation of subgrid cloud and precipitation processes within RegCM," *Journal of Geophysical Research D: Atmospheres*, vol. 105, no. 24, pp. 29579–29594, 2000.

[52] R. E. Dickinson, S. A. Henderson, and P. Kennedy, "Bio-sphere-atmosphere transfer scheme (BATS) version 1e as coupled to the NCAR community climate model," Tech. Rep. TN-387+STR, National Center for Atmospheric Research, Boulder, Colorado, 1993.

[53] F. Giorgi, R. Francisco, and J. S. Pal, "Effects of a sub-grid scale topography and landuse scheme on surface climate and hydrology. I. Effects of temperature and water vapor disaggregation," *Journal of Hydrometeorogy*, vol. 14, pp. 317–333, 2003.

[54] A. L. Steiner, J. S. Pal, S. A. Rauscher et al., "Land surface coupling in regional climate simulations of the West African monsoon," *Climate Dynamics*, vol. 33, no. 6, pp. 869–892, 2009.

[55] A. B. Tawfik and A. L. Steiner, "The role of soil ice in land-atmosphere coupling over the United States: a soil moisture-precipitation winter feedback mechanism," *Journal of Geophysical Research D: Atmospheres*, vol. 116, no. 2, Article ID D02113, 2011.

[56] K. W. Oleson, Y. Dai, G. Bonan et al., "Technical description of the Community Land Model," National Center for Atmospheric Research Tech Note NCAR/TN-461+STR, NCAR, Boulder, Colo, USA, 2004.

[57] K. W. Oleson, G.-Y. Niu, Z.-L. Yang et al., "Improvements to the Community Land Model and their impact on the hydrologic cycle," *Journal of Geophysical Research G: Biogeosciences*, vol. 113, no. 1, 2008.

[58] X. Zeng and A. Beljaars, "A prognostic scheme of sea surface skin temperature for modeling and data assimilation," *Geophysical Research Letters*, vol. 32, no. 14, pp. 1–4, 2005.

[59] X. Zeng, M. Zhao, and R. E. Dickinson, "Intercomparison of bulk aerodynamic algorithms for the computation of sea surface fluxes using TOGA COARE and TAO data," *Journal of Climate*, vol. 11, no. 10, pp. 2628–2644, 1998.

[60] F. Solmon, F. Giorgi, and C. Liousse, "Aerosol modelling for regional climate studies: application to anthropogenic particles and evaluation over a European/African domain," *Tellus, Series B: Chemical and Physical Meteorology*, vol. 58, no. 1, pp. 51–72, 2006.

[61] A. S. Zakey, F. Solmon, and F. Giorgi, "Implementation and testing of a desert dust module in a regional climate model," *Atmospheric Chemistry and Physics*, vol. 6, no. 12, pp. 4687–4704, 2006.

[62] A. S. Zakey, F. Giorgi, and X. Bi, "Modeling of sea salt in a regional climate model: fluxes and radiative forcing," *Journal of Geophysical Research D: Atmospheres*, vol. 113, no. 14, Article ID D14221, 2008.

[63] B. Laurent, B. Marticorena, G. Bergametti, J. F. Léon, and N. M. Mahowald, "Modeling mineral dust emissions from the Sahara desert using new surface properties and soil database," *Journal of Geophysical Research D: Atmospheres*, vol. 113, no. 14, Article ID D14218, 2008.

[64] J. F. Kok, "A scaling theory for the size distribution of emitted dust aerosols suggests climate models underestimate the size of the global dust cycle," *Proceedings of the National Academy of Sciences of the United States of America*, vol. 108, no. 3, pp. 1016–1021, 2011.

[65] S. W. Hostetler, G. T. Bates, and F. Giorgi, "Interactive coupling of a lake thermal model with a regional climate model," *Journal of Geophysical Research*, vol. 98, no. 3, pp. 5045–5057, 1993.

[66] E. E. Small, L. C. Sloan, S. Hostetler, and F. Giorgi, "Simulating the water balance of the Aral Sea with a coupled regional climate-lake model," *Journal of Geophysical Research D: Atmospheres*, vol. 104, no. 6, pp. 6583–6602, 1999.

[67] E. Coppola, F. Giorgi, L. Mariotti, and X. Bi, "RegT-band: a tropical band version of RegCM4," *Climate Research*, vol. 52, no. 1, pp. 115–133, 2012.

[68] M. O. Adeniyi, "Sensitivity of different convection schemes in RegCM4.0 for simulation of precipitation during the Septembers of 1989 and 1998 over West Africa," *Theoretical and Applied Climatology*, vol. 115, no. 1-2, pp. 305–322, 2014.

[69] M. Yu and G. Wang, "Impacts of bias correction of lateral boundary conditions on regional climate projections in West Africa," *Climate Dynamics*, vol. 42, no. 9-10, pp. 2521–2538, 2014.

[70] S. Uppala, D. Dee, S. Kobayashi, P. Berrisford, and A. Simmons, "Towards a climate data assimilation system: status update of ERA-Interim," *ECMWF Newsletter*, vol. 115, no. 7, pp. 12–18, 2008.

[71] R. W. Reynolds, N. A. Rayner, T. M. Smith, D. C. Stokes, and W. Wang, "An improved in situ and satellite SST analysis for climate," *Journal of Climate*, vol. 15, no. 13, pp. 1609–1625, 2002.

[72] R. F. Adler, G. J. Huffman, A. Chang et al., "The version 2 global precipitation climatology project (GPCP) monthly precipitation analysis (1979-present)," *Journal of Hydrometeorology*, vol. 4, pp. 1147–1167, 1979.

[73] I. Harris, P. D. Jones, T. J. Osborn, and D. H. Lister, "Updated high-resolution grids of monthly climatic observations—the CRU TS3.10 Dataset," *International Journal of Climatology*, vol. 34, no. 3, pp. 623–642, 2014.

[74] T. D. Mitchell and P. D. Jones, "An improved method of constructing a database of monthly climate observations and associated high-resolution grids," *International Journal of Climatology*, vol. 25, no. 6, pp. 693–712, 2005.

[75] C. J. Schreck III and F. H. M. Semazzi, "Variability of the recent climate of Eastern Africa," *International Journal of Climatology*, vol. 24, no. 6, pp. 681–701, 2004.

[76] D. P. Dee, S. M. Uppala, A. J. Simmons et al., "The ERA-Interim reanalysis: configuration and performance of the data assimilation system," *Quarterly Journal of the Royal Meteorological Society*, vol. 137, no. 656, pp. 553–597, 2011.

[77] E. Kalnay, M. Kanamitsu, R. Kistler et al., "The NCEP/NCAR 40-year reanalysis project," *Bulletin of the American Meteorological Society*, vol. 77, no. 3, pp. 437–471, 1996.

[78] Intergovernmental Panel on Climate Change (IPCC), *Climate Change 2007: Impacts, Adaptation and Vulnerability. Contribution of Working Group II to the Fourth Assessment Report of the Intergovernmental Panel on Climate Change*, edited by M. L. Parry, O. F. Canziani, J. P. Palutikof, P. J. van der Linden and C. E. Hanson, Cambridge University Press, Cambridge, UK, 2007.

[79] E. A. Afiesimama, J. S. Pal, B. J. Abiodun, W. J. Gutowski Jr., and A. Adedoyin, "Simulation of West African monsoon using the RegCM3. Part I: model validation and interannual variability," *Theoretical and Applied Climatology*, vol. 86, no. 1–4, pp. 23–37, 2006.

[80] E. Lu, "Monitoring and maintenance of a cold-season drought," in *Science and Technology Infusion Climate Bulletin, NOAA's National Weather Service . The 37th NOAA Annual Climate Diagnostics and Prediction Workshop*, pp. 99–102, Fort Collins, Colo, USA, 2012.

[81] R. G. Barry and R. J. Chorley, *Atmosphere, Weather and Climate*, 8th edition, 2003.

[82] B. A. Ogwang, T. Guirong, and C. Haishan, "Diagnosis of September-November drought and the associated circulation anomalies over Uganda," *Pakistan Journal of Meteorology*, vol. 9, no. 17, pp. 11–24, 2012.